ICSV13 - Vienna
The Thirteenth International Congress on Sound and Vibration
Vienna, Austria, July 2-6, 2006

Application of Optimized Compact Finite Difference Schemes on Uneven Grid to the Computation of Acoustic Wave Propagation

Reima Iwatsu*[1], Hideo Tsuru[2], and Kunikazu Hirosawa[2]

*[1] Department of Mechanical Engineering, Tokyo Denki University
2-2 Kanda, Chiyoda-ku Tokyo 101-8457, Japan
[2]Nittobo Acoustic Engineering Corporation
1-21-10 Midori, Sumida-ku Tokyo 130-0021, Japan
iwatsu@cck.dendai.ac.jp (e-mail address of lead author)

Abstract

Compact schemes and linear multi-step methods are applied to the wave equation with an intention to extend the applicability of the conventional FDTD method to complex geometries. Fourth-order compact finite difference scheme on unevenly spaced staggered mesh is utilized for the spatial discretization. System of equations is integrated in time by using linear multi-step methods that use half-node arrangement in time. The coefficients of these time stepping methods are chosen to assure appropriate accuracy for the amplification factor and phase error over the frequency of interest while the whole time integration yields a stable solution. Proposed method is applied to several benchmark problems and the results show better resolution capability compared to the conventional method.

INTRODUCTION

It appears that numerical simulation of sound wave propagation in rooms is now realistic at least for low frequencies. Two methods are commonly used for the analyses of room acoustics: boundary element method and finite difference method. The latter method is easy to code, and straightforward to obtain pressure distribution as time progresses. The cell centered finite difference scheme of second-order and the Leap-Frog method are commonly used in the computation in time domain. Combination of these amazingly simple schemes does produce stable and moderately accurate solutions often sufficient for industrial use. This comfortable situation encounters difficulty however, when we have to analyze rooms with non-parallel walls, desks and furniture, not to mention that reflective conditions on the material surface are not exactly known. A remedy may be to use unevenly spaced grid points to model complex boundary shapes and to employ finite difference schemes for uneven mesh. In the present report, compact finite difference schemes [4] extended to uneven grid spacing are utilized and linear multi-step methods are tested for time marching. The coefficients of multi-step methods are optimized so as to maximize the accuracy limit and stability limit of the effective angular frequency of the schemes.

NUMERICAL METHOD

The problem to be solved is the initial-boundary value problem of linear wave equation in three-dimensions. For the purpose of explanation, equations are written for scalar variables, however extension to more than two-dimensions is straightforward.

$$f_{tt} = H(f,t), \quad f(x,t=0) = f_0, \tag{1}$$

where f is either the velocity of the fluid or the pressure, H is the source term $c^2 f_{xx}$, c is a constant sound velocity, f_0 is the initial value, and an appropriate boundary conditions are imposed in addition. In the FDTD procedure, intermediate variable g is introduced and the above equation is integrated in a form of two separate advection equations.

$$f_t = F(g,t), \quad g_t = G(f,t), \tag{2}$$

where the couple f, g stands for the pressure and velocity or the velocity and pressure, the source terms $F = -cg_x$, and $G = -cf_x$. In this form of equations, additional initial and boundary values are required for the new variable g. Naturally when the two equations are combined, the wave equation is retrieved since $H \equiv FG = GF$.

Spatial Discretization

For the evaluation of first derivative, compact finite difference scheme for cell centered uneven mesh is used for inner grid points. Let us refer this scheme as CDuns(3,2).

$$\alpha f'_{i-1} + f'_i + \beta f'_{i+1} = a(f_{i+\frac{1}{2}} - f_{i-\frac{1}{2}}) + \epsilon \tag{3}$$

For the boundary points (at $i = i_{min}$), either of the following schemes, A (eq.4) or B (eq.5) is used, depending on the location of half-nodes.

$$f'_i + \beta f'_{i+1} = a(f_{i+\frac{1}{2}} - f_{i-\frac{1}{2}}) + b(f_{i+\frac{3}{2}} - f_{i-\frac{1}{2}}) + \epsilon \tag{4}$$

$$f'_i + \bar{\beta} f'_{i+1} = \bar{a}(f_{i+\frac{3}{2}} - f_{i+\frac{1}{2}}) + \bar{b}(f_{i+\frac{5}{2}} - f_{i+\frac{1}{2}}) + \epsilon \tag{5}$$

Coefficients of above schemes are numerically determined form given mesh intervals. For sufficiently smooth meshes, schemes CDuns(3,2), and the boundary schemes A, B are fourth-order and third-order respectively. When the grid spacing is uniform, CDuns(3,2) retrieves the Padè scheme.

Time Integration

For the time integration of advection equations, liner multi-step method of the following form (M_s) is used.

$$f^{n+1} = f^n + \Delta t \sum_{j=0}^{s-1} b_j F^{n+\frac{1}{2}-j} + \epsilon \tag{6}$$

where ϵ is the leading term of the error. When $s = 3$, by requiring second-order, coefficients are obtained as $b_1 = 2-2b_0$, $b_2 = b_0-1$ and the error $\epsilon = \frac{\Delta t^2}{24}(24b_0-25)f_{ttt}$. When $s = 4$, they are $b_1 = -3b_0 + 73/24$, $b_2 = 3b_0 - 37/12$, $b_3 = 25/24 - b_0$ and $\epsilon = \frac{\Delta t^3}{12}(12b_0 - 13)f_{tttt}$. It may be unnecessary to note that for $s = 3$ and $b_0 = 1$, time integration is reduced to the Leap-Frog method. The value of parameter b_0 will be determined later.

After the first integration M_s, it is followed by the second integration M_r

$$g^{n+1} = g^n + \Delta t \sum_{k=0}^{r-1} c_k G^{n+\frac{1}{2}-k} + \epsilon. \tag{7}$$

Equations (6) and (7) integrate the wave equation from time level n to $n+1$

$$f^{n+1} = 2f^n - f^{n-1} + \Delta t^2 \sum_{l=0}^{q-1} d_l H^{n-l} + \epsilon. \tag{8}$$

where $q = s + r - 1$ and $d_l = \sum_{j=0}^{l} b_{l-j} c_j$. If we refer the above method as M_q^2, it is obvious that $M_{r+s-1}^2 \equiv M_r \cdot M_s$. Stability and accuracy of M_q^2 is analyzed in the following. Since analyses of M_q^2 involves too many free parameters, only the cases, $M_3^2 \equiv M_3 \cdot M_1$, $M_4^2 \equiv M_4 \cdot M_1$ and $M_5^2 \equiv M_3 \cdot M_3$ are treated in the present study.

RESULTS

In the following, numerical error of CDuns(3,2) combined with boundary schemes A and B are estimated first for a sine wave. Then angular frequency of the compact schemes is analyzed for non-uniform mesh. Optimization of multi-step time integration is described next, and finally proposed method is applied to several benchmark problems.

Estimation of spatial error

Sine wave $f(x) = \sin(\alpha x), \alpha = \pi$ is chosen as a test function to estimate numerical error of CDuns(3,2)+ boundary schemes A or B. By varying the number of mesh points n, average error and the maximum error in the first derivative are plotted as functions of n and x in Fig. 1 for a hyperbolic tangent mesh. The fourth-order accuracy is actually realized and the maximum error always appears on the boundaries. Although both boundary schemes A and B have same order of accuracy, maximum error of scheme A is smaller than B when n is large. Modest accuracy of 10^{-3} in the first derivative is achieved when $n-1 \sim 8$ for both cases A and B, i.e. $\alpha\Delta x \sim 0.39$. This means that with this tolerance, approximately 8 points are necessary within a wave length.

For uniform mesh, CDuns(3,2) has a real angular frequency. The angular frequency of CDuns(3,2) is plotted in Fig. 2 for a power low grid $x_i = r^i$ to show the effect of non-uniform mesh. Plots in Fig. 2 indicate that the choice of $r = 1.2$ causes a phase error of $2.5 \cdot 10^{-2}$ for $\alpha\Delta x \leq \pi$. Analysis on the effect of ratio of grid spacing r on the angular frequency provides a guideline on how to distribute grid points.

Optimization of Multi-Step Methods

Multi-step methods for advection equation: The angular frequency $\bar{\omega}$ of multi-step methods $M_s, s = 3, 4$ (eq.6) is obtained as follows, by using the Laplace transform and assuming that $f = 0$ for $t \leq 0$.

$$\bar{\omega}\Delta t = \frac{2sin(\frac{\omega\Delta t}{2})}{\sum_{j=0}^{s-1} b_j e^{ij\omega\Delta t}} \tag{9}$$

According to [1], coefficients of the methods are optimized by requiring that deviation in the angular frequency is minimized over frequencies of interest,

$$E_1 = \int_{-\eta}^{\eta} \left(\sigma Re(\bar{\omega}\Delta t - \omega\Delta t)^2 + (1-\sigma) Im(\bar{\omega}\Delta t - \omega\Delta t)^2\right) d(\omega\Delta t), \quad \frac{dE_1}{db_0} = 0 \tag{10}$$

where $\sigma = 0.36$ was used as in [1]. By assuming $\eta = 0.5$ for $s = 3$ and $\eta = \pi/2$ for $s = 4$, the following values are obtained: $b_0 = 1.03340232$ for $s = 3$, $b_0 = 1.0843831$ for $s = 4$. The Leap-Frog method M_1 is a special case where $Im(\bar{\omega}\Delta t) = 0$. Optimized version of M_3 and M_4 introduce a slight error in the imaginary part. In turn, they attain more accurate real part over a wider range of angular frequency than M_1. To obtain a better understanding, E_1 is plotted as a function of b_0 in Fig. 3 for $s = 3$. As shown in the figure, the optimal of b_0 varies as η is varied. The value of η should be chosen by considering the stability limit. In the present study, it was determined from the accuracy and stability limit of the combined method, M_q^2. Combined multi-step methods for wave equation are now described in the following.

Multi-step methods for wave equation: The stability of time integration methods M_q^2 is analyzed by considering the amplification factor of the methods. Numerical amplification factor of M_q^2 is compared with the exact amplification factor $r_{exact} = e^{-i\omega\Delta t}$,

$$\frac{r_{num}}{r_{exact}} = 2e^{i\omega\Delta t} - e^{i2\omega\Delta t} - (\omega\Delta t)^2 \sum_{l=0}^{q-1} d_l e^{i(l+1)\omega\Delta t}. \tag{11}$$

In accordance to the notation of [2], above ratio is denoted as $re^{-i\delta}$, where r is the ratio of amplification factors and δ the phase error. The stability limit is defined as the maximum angular frequency $\omega\Delta t(= w$ in Figs. 3 and 4) where $|r| \leq 1$ is satisfied and denoted by a sign R in the figures. Accuracy limit for the amplification factor and phase error are defined as the maximum angular frequencies where $||r| - 1| \leq 10^{-3}$ and $|\delta| \leq 10^{-3}$ holds. In Figs. 3 and 4, they are denoted as L and I respectively. The results are shown first in Fig. 3 (right) for M_3. In Fig. 4, accuracy and stability limit for $M_q^2, q = 3, 5$ are shown as functions of d_0. Recommended ranges for the value of d_0 are $1.03 \leq d_0 \leq 1.083$, $\omega\Delta t \leq 0.4$ for M_3^2, $1.04 \leq d_0 \leq 1.135$, $\omega\Delta t \leq 0.4$ for M_4^2 and $1.28 \leq d_0 \leq 1.37$, $\omega\Delta t \leq 0.45$ for M_5^2. In summary, it is confirmed that M_s and $M_s \cdot M_r$ are stable with respect to the previously obtained optimal values of b_0.

Benchmark Problems

One-dimensional wave propagation [3]: The solution at $t = 400$ of $f_t + f_x = 0$ where $f(0) = \frac{1}{2}\exp\left(-\text{in}(2)\left(\frac{x}{3}\right)^2\right)$, $-20 \leq x \leq 450$, $\Delta x = 1.0$ was computed by using conventional method ($= M_1 \cdot M_1$) and optimized $M_3 \cdot M_3$ (Fig. 5). To see whether multi-step methods improve the accuracy of numerical solutions, deviation of numerical solution from the exact solution $dev_2 = \sum |f_n - f_{exact}|^2$ versus b_0 is plotted in Fig. 6. It is readily seen that error of multi-step methods are two-order of magnitude smaller than the conventional method.

Three-dimensional wave scattered by a sphere: Sound wave scattered by a sphere is computed and calculated pressure is compared with the exact solution written in a form of infinite series expansion. The radius of sphere is 0.2 (m) and the spherical shape is expressed by masking the orthogonal mesh. Sound source is located at a point 1 (m) apart from the center of the sphere. The average mesh spacing is 0.02 (m) in all directions and a total of 101^3 grid points are used. Solutions are obtained on both uniform and non-uniform meshes. For the non-uniform mesh, the minimum grid spacing is 0.0083 (m). Discrete time interval is fixed at $\Delta t = 0.01$ (msec). Sound frequency is changed from 500 (Hz), 1000 (Hz) to 2000 (Hz). The computed pressure in the frequency domain is shown in Fig. 7 (upper left) in the unit of (dB) for the compact schemes combined with multi-step method ($M_3 \cdot M_3$ with $b_0 = 1.04$ for both velocity and pressure integration). It was noted that the maximum error in the numerical solution by FTDT is 5 (dB), while the maximum error is decreased to 3 (dB) when ED2 is replaced to CD4uns(3,2) (Fig. 7 upper right). Further replacement of $M_1 \cdot M_1$ to $M_3 \cdot M_3$ decreases 0.3 (dB) (Fig.7 lower). Thus improvement is observed for optimized version of the multi-step method.

SUMMARY

Compact finite difference schemes on cell centered uneven mesh and optimized multi-step methods are applied to the computation of sound wave equation. Proposed methods produced numerical solution of good quality for benchmark problems. As to the future plans, the following items will be treated.

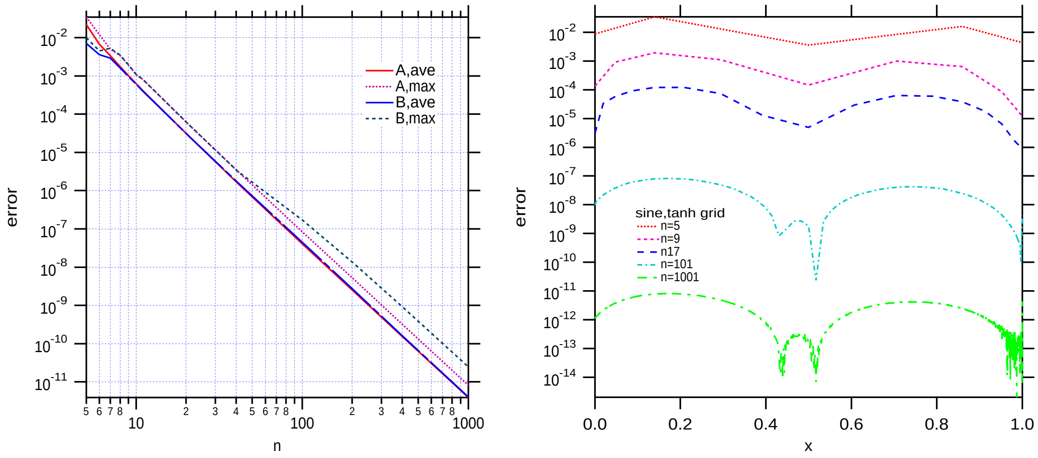

Figure 1: Error vs number of grid points n (left), error distribution for hyperbolic mesh, CDuns(3,2) + A,B

Application of compact scheme which uses four grid points on the right hand side, i.e. CDuns(3,4) will be studied. By requiring fourth-order accuracy, one parameter is undetermined in the coefficients and this parameter is used to optimize the wave propagation property of the scheme for a given non-uniform mesh point distribution.

In the present study, optimized parameter is proposed for one-parameter family of three and four step methods $M_s, s = 3, 4$ for advection equation and three and five step methods $M_q^2, q = 3, 5$ for wave equation. It is now planned further to explore the combination of M_3 and M_4. These methods result in $M_6^2 \equiv M_3 \cdot M_4$ and $M_7^2 \equiv M_4 \cdot M_4$.

REFERENCES

References

[1] C.K.W.Tam, J.C.Webb, "Dispersion-relation-preserving schemes for computational acoustics", J. Comput. Phys., **107**, 262-281 (1993)

[2] F.Q. Hu, M.Y. Hussaini, J.L. Manthey, "Low-dissipation and low-dispersion Runge-Kutta schemes for computational acoustics", J. Comput. Phys., **124**, 177-191 (1996)

[3] J.C. Hardin *et al.* (Eds.) "ICASE/LaRC Workshop on benchmark problems in computational aeroacoustics," NASA CP-3300, (1995)

[4] S.K. Lele, "Compact finite difference schemes with spectral-like resolution", J. Comput. Phys., **103**, 16-42 (1992)

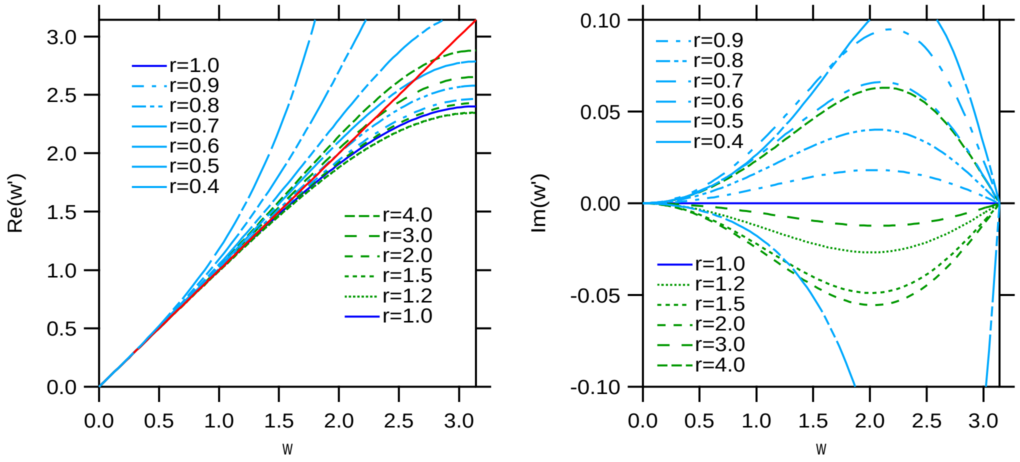

Figure 2: Effective frequency of CDuns(3,2) for non-uniform power-low mesh $x_i = r^i$; Left: real part, right: imaginary part

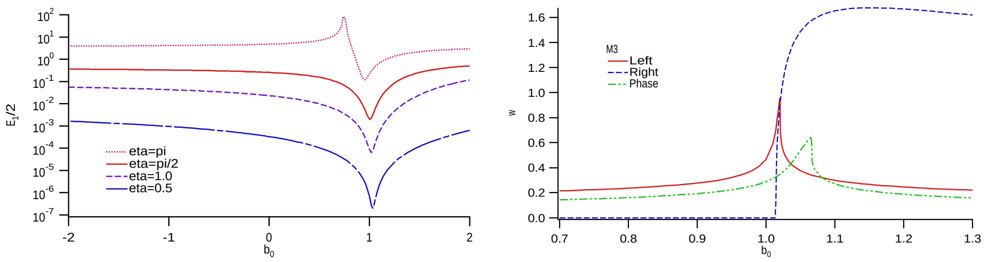

Figure 3: Deviation in the angular frequency E_1 of multi-step method M_3 as a function of b_0 (Left), accuracy limit of amplification factor L, phase error I and stability limit R (right) of M_3 as a function of b_0

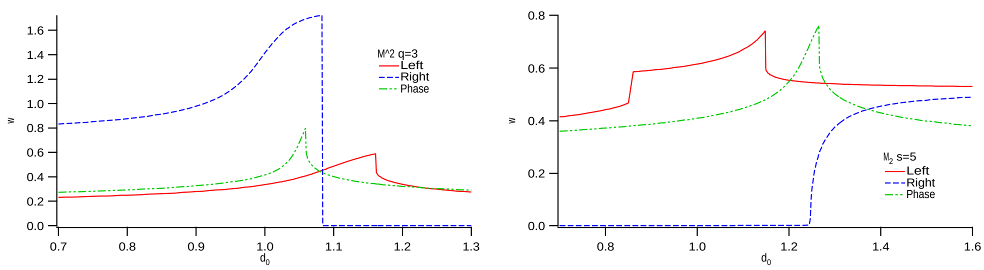

Figure 4: Accuracy limit of amplification factor L, phase error I and stability limit R for M_3^2 and M_5^2

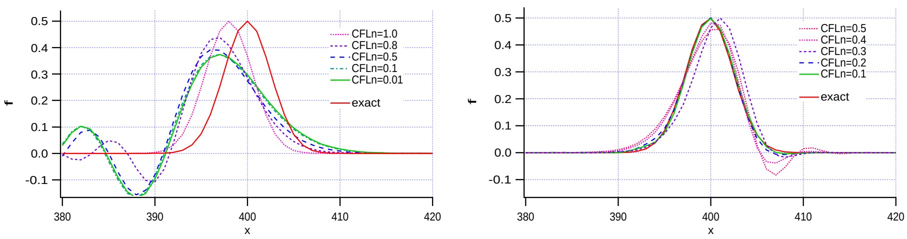

Figure 5: Numerical solution at $t = 400$ obtained by FDTD (left) and $M_3 \cdot M_3$ (right)

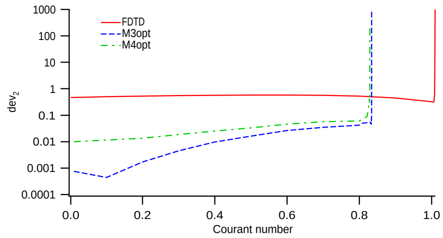

Figure 6: Error dev_2 vs Courant number for FDTD, $M_3 \cdot M_3$ and $M_4 \cdot M_4$

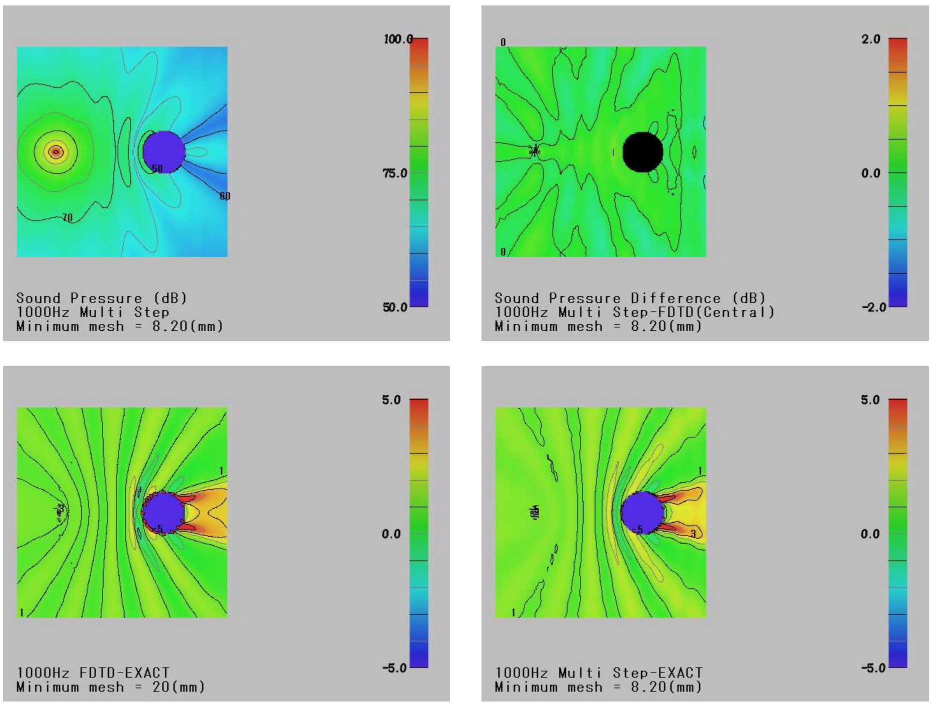

Figure 7: Sound pressure distribution in the frequency domain at 1000 (Hz) and difference in p between FDTD and present (upper), Δp (deviation from the exact solution) shown in (dB) for FDTD + CDuns(3,2) and present method (lower)